

## CHAPTER II

### LITERATURE REVIEW

#### 2.1 Reduced Graphene Oxide

In graphite, the graphene layers have strong cohesive force hence it is difficult to get exfoliated graphene sheets. To reduce the cohesive force between the graphene sheets and also to impart specific interaction with the host polymer matrix functionalization of graphene is essential. Graphite upon oxidation produces graphite oxide (GO) having hydrophilic functional groups (-OH, epoxide, -COOH) which promotes the intercalation of water molecules into the gallery and the graphene sheets can be easily detached from each other by sonication, thus producing highly dispersible GO sheets in aqueous medium. The GO is electrically insulating but become conducting when it is reduced to produce reduced graphene oxide (RGO) by sodium borohydride or hydrazine hydrate (Rama and Arun, 2013).

In 2013, Chen *et al.*, developed the improved Hummers method without using  $\text{NaNO}_3$  for synthesis of GO. This improved method eliminates the generation of toxic gasses and simplifies the procedure of purifying waste liquid, thus decreasing the cost of GO synthesis. The prepared GO product is nearly the same characteristic and can be prepared in large scale. After synthesis GO, sodium borohydride was used to be a reducing agent in order to increase the surface area (Vilian *et al.*, 2014)

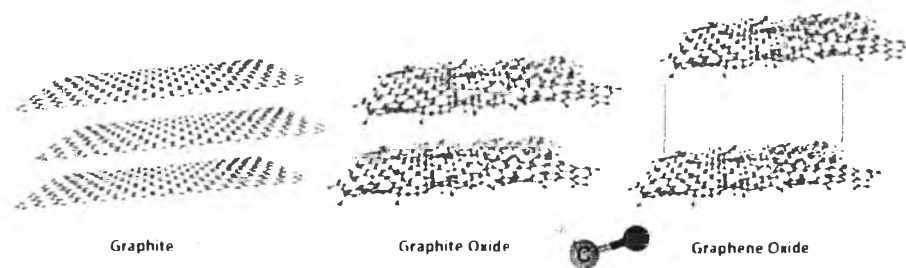


**Figure 2.1** Illustration of the GO synthesis from the graphite particles

(Tugral *et al.*, 2014).

Perera *et al.* prepared graphene by using alkaline hydrothermal synthesis and studied as electrode for symmetric supercapacitors. They compared the performance of hGO (alkaline hydrothermal synthesis of GO) and rGO (hydrazine reduction of GO). Figure 2.2 show the XRD pattern of graphite and GO. Graphite powder exhibits a strong (002) reflection at  $26.5^\circ$ . After oxidation of graphite to GO, the (002) diffraction peak shifts to a lower  $2\theta$  angle ( $10.8^\circ$ ). This indicates the GO sheets are separated due to the covalently bonded oxygen (Moon *et al.*, 2010). The oxidation of graphite to GO disrupts the conjugation of the graphene structure resulting a decrease in electronic conductivity. Hydrazine has been widely used to reduce GO to graphene and restore the conjugated  $sp^2$  network. It was reported that hydrazine reduced GO exhibit higher electronic conductivities (Moon *et al.*, 2010) than that of GO and can be used to prepare films and composites with different materials for energy conversion and storage applications Yoo *et al.*, 2011 and Gwon *et al.*, 2011. Although hydrazine is the most common reducing agent used to prepare reduced GO, high toxicity and hazardous bi-products greatly limits its use for the large-scale preparation of graphene for industrial applications. The irreversible aggregation of graphene layers in the presence of excess hydrazine has also been reported. In order to overcome these limitations, we prepared deoxygenated GO by an alkaline hydrothermal process (hGO) at  $120^\circ\text{C}$ , which was expected to deoxygenate GO to a higher degree than either just washing or the low temperature alkaline treatment previously reported (Fan *et al.*, 2008). Figure 2a shows the XRD patterns for the hydrazine reduced GO (rGO) and hGO. The interlayer distance of rGO obtained from (002) reflection of the XRD pattern at  $23.6^\circ$  was  $\sim 0.37$  nm. The decrease in interlayer spacing between individual graphene sheets is attributed to the van der Waals interaction between  $sp^2$  hybridized carbon frame-work that was restored during the chemical reduction. The XRD pattern of hGO also exhibits a (002) reflection at  $23.9^\circ$  corresponding to the interlayer spacing of  $\sim 0.37$  nm. The broad XRD peak of the hGO suggests these stacked graphene sheets are few layers thick .

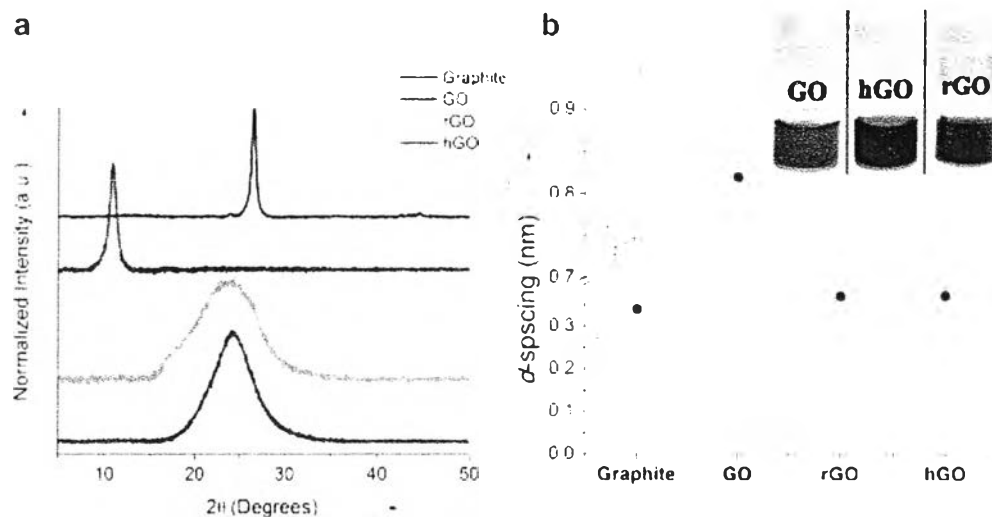


**Figure 2.2** (a) XRD patterns of Graphite after oxidation to GO and followed by the reduction with hydrazine and alkaline hydrothermal treatment. (b) d-spacing of each samples (digital photographs of aqueous dispersions of GO and hGO sample inset) (Perera *et al.*, 2012).

FTIR spectroscopy was used to investigate different bondings in GO and rGO. Figure 2.3 shows the FTIR absorbance spectra (mixed with KBr) of GO and rGO. There were a number of functional groups in GO and rGO. A broad peak with the maximum at  $3400\text{ cm}^{-1}$  in the lower spectrum was identified to be due to the C-OH bonding from hydroxyls and trapped water molecules in the GO sample. The presence of trapped water molecules between the GO layers or on the surface of the GO sheets broadens the C-OH band. For reduced GO, upper spectrum, this broad peak is changed to a narrower peak for C-OH bonding and a sharp peak at  $2950\text{ cm}^{-1}$  for C-H bonds. This change is due to the partial removal of hydroxyl groups and water molecules by chemical reduction. C=O from carbonyl or carboxyl groups ( $1734\text{ cm}^{-1}$ ), C=C bonds from unoxidized  $\text{sp}^2$  graphite domains ( $1627\text{ cm}^{-1}$ ), O-H from carboxyl ( $1410\text{ cm}^{-1}$ ), C-C bonds from epoxy ( $1230\text{ cm}^{-1}$ ) and C-O bonds from carbonyl ( $1060\text{ cm}^{-1}$ ) were also observed for GO sample. After chemical reduction, C=O bond in  $1734\text{ cm}^{-1}$  is disappeared; C-O-C bonds in  $1230\text{ cm}^{-1}$  and C-O bonds in  $1060\text{ cm}^{-1}$  is sharpened and one peak from C-O-C bonds is observed in  $800\text{ cm}^{-1}$ .

In GO, epoxides were present at a lower concentration in comparison to hydroxyls which is typical in GO samples. As can be seen in Figure 2.3, the removal of hydroxyls using chemical reduction is more effective than epoxides which is probably due to the weaker bonding energy of hydroxyl groups. However, C-O-C bonds and C-O stretching vibrations become sharper, which are caused by remaining epoxide, carbonyl and carboxyl groups even after reduction (Choi *et al.*, 2010).

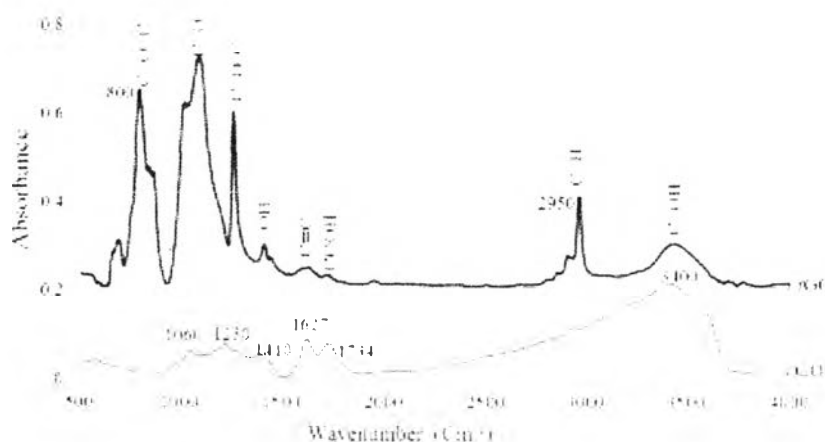


**Figure 2.3** FTIR spectra of GO (bottom) and rGO (up).

## 2.2 Polyelectrolyte

The polymers that contain a net negative or positive charge at pH are called polyelectrolytes. Depending on their ionization, they are generally soluble in water. Their solubility is driven by the electrostatic interactions between water and the charged monomer. Examples of such polymers include DNA, protein, certain derivatives of cellulose polymers and carragenan.

The polyelectrolytes are classified into various types. Based on origin they are classified as natural polyelectrolytes, synthetic polyelectrolytes and chemically modified biopolymers. Based on composition they are homopolymers and copolymers. Based on molecular architecture linear, branched and cross linked.

Based on electrochemistry they are classified as polyacids/polyanions, polybases/polycations and polyampholytes.

- 1) Polydiallyldimethylammonium chloride (PDADMAC) structure was shown as Figure 2.4

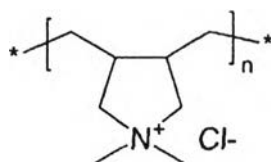


**Figure 2.4** Polydiallyldimethylammonium chloride (PDADMAC)

- 2) Polystyrene sulfonic acid (PSS) structure was shown as Figure 2.5

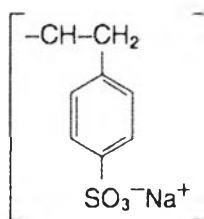


**Figure 2.5** Polystyrene sulfonate (PSS)

### 2.3 Layer-by-layer (LbL) of Polyelectrolyte Multilayers

Polyelectrolyte multilayers (PEMs) are a versatile type of thin film that is created via layer-by-layer assembly of positively and negatively charged polymers (shown in Figure 2.6) from aqueous solutions. Precise control of the PEM thickness, chemical functionality, and molecular architecture is made possible by changing the polyelectrolytes and assembly conditions during film growth, allowing films to be designed with properties suitable for a given application.

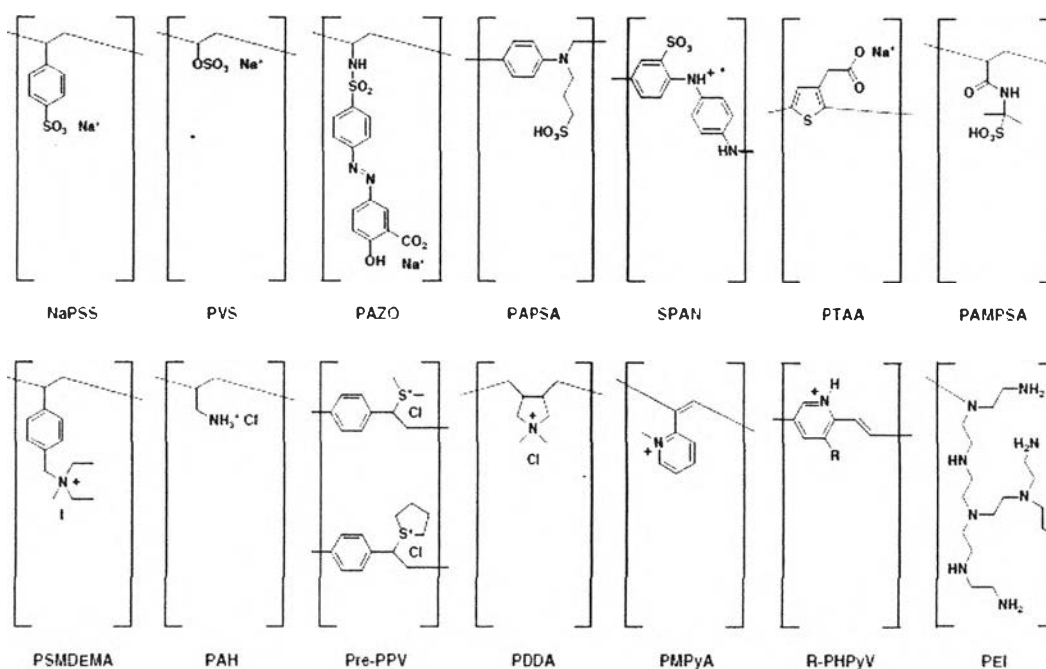


**Figure 2.6** Example of polyions used for multilayer fabrication.

The adsorption of organic molecules to interfaces is offering a variety of possibilities for the design of novel materials with structures defined on a nanometer scale. So-called “self-assembly”- processes, employing the self-organization of molecules at interfaces as a result of for example hydrophobic or electrostatic interactions can be employed to produce layered materials.

In the case of polyelectrolytes the electrostatic interaction can be employed by immersions into solutions, alternating between polycations and polyanions. When a substrate with a negative surface charge is immersed into a solution with positively charged polyelectrolyte chains, the electrostatic attraction leads to an irreversible binding of the chain to the surface, while the counterions remain in the electric double layer. Thus, a monomolecular layer with a thickness on the order of one nanometer is formed. Under suitable conditions, the net surface charge is positive, such that as a next step, a negatively charged polyion can be adsorbed by immersion into a solution of polyanions. The counterions remain in the solution due to their large entropic contributions. Repeating this procedure of immersion into solutions of

chains of alternating charge is a simple way of forming a material with a large variability concerning different molecular constituents that can be employed.

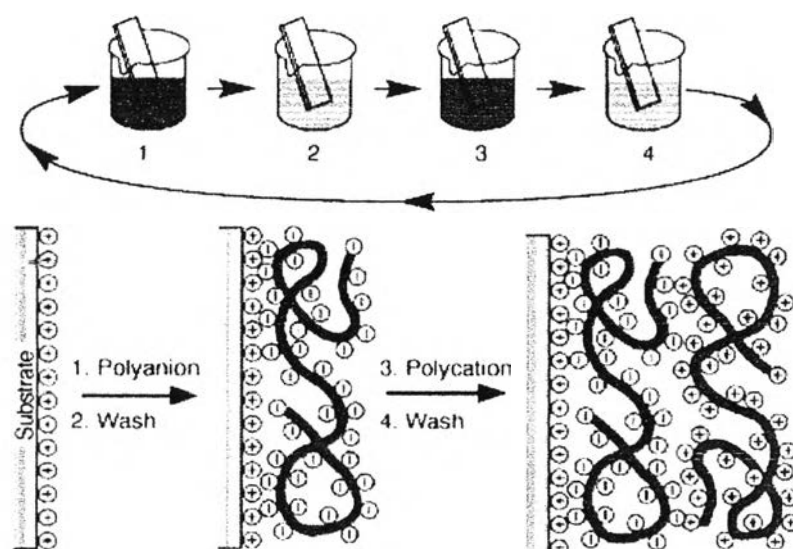


**Figure 2.7** The layer-by-layer (LbL) assemble technique (Decher *et al.*, 1997).

The layer-by-layer (LbL) technique as shown in Figure 2.7, first introduced by Iler<sup>1</sup> in 1966 and re-established and refined by Decher in the 1990s, has shown great success in fabricating polymer thin films with controllable compositions, structures and properties.

In 2004, Gong and Gao found an important phenomenon of the multilayer compression, which can yield geometric patterns on the multilayers without an alteration of their surface chemistry. The overall compression degree of poly(styrene sulfonate) (PSS)/PDADMAC multilayers is as high as 70–90 % depending on the film thickness, and thereby the absolute height of the formed patterns increases along with the layer number and concentration of NaCl used during the assembly as shown in Figure 2.8.

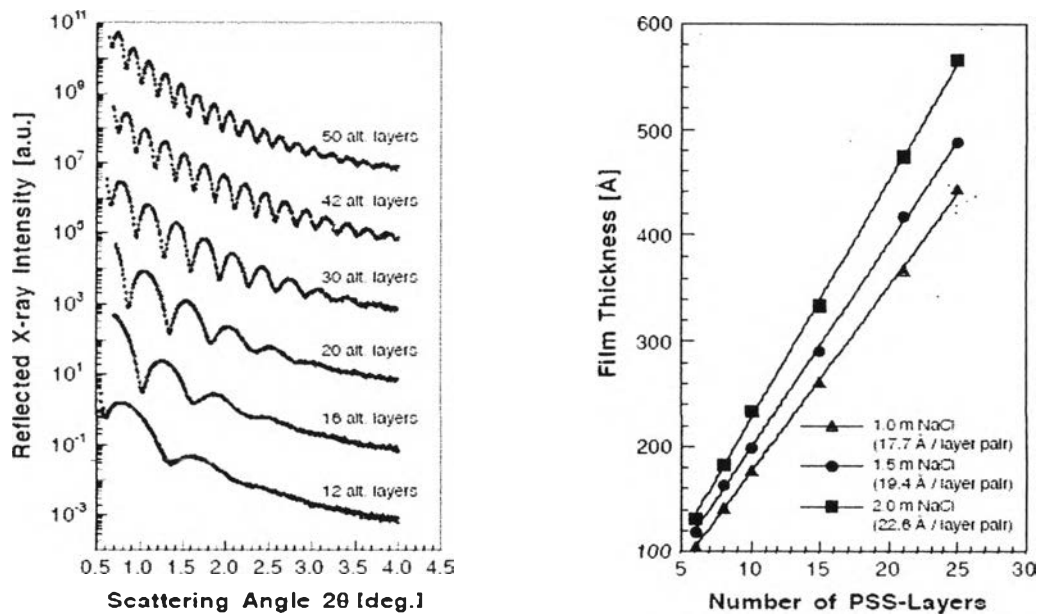


**Figure 2.8** Fine-tuning the film thickness by ionic strength by X-ray reflectometry (Decher *et al.*, 1992).

#### 2.4 Layer-by-layer (LbL) of RGO/PDADMAC

Zhang *et al.* fabricated a resistive-type humidity sensor with RGO/PDADMAC nanocomposite film by using LbL nano self-assembly method as shown in Figure 2.9. The film sensor was fabricated on flexible polyimide substrate. First, two bi-layers of PDADMAC/PSS were self-assembled as precursor layers for charge enhancement, followed by the alternative sequence of the immersion into PDADMAC and GO suspensions for five repetitive cycles as shown in Figure 2.10.



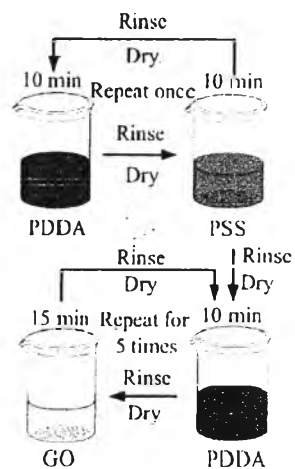


**Figure 2.9** Layer-by-layer (LbL) fabrication process of PDADM/RGO nanocomposite film.

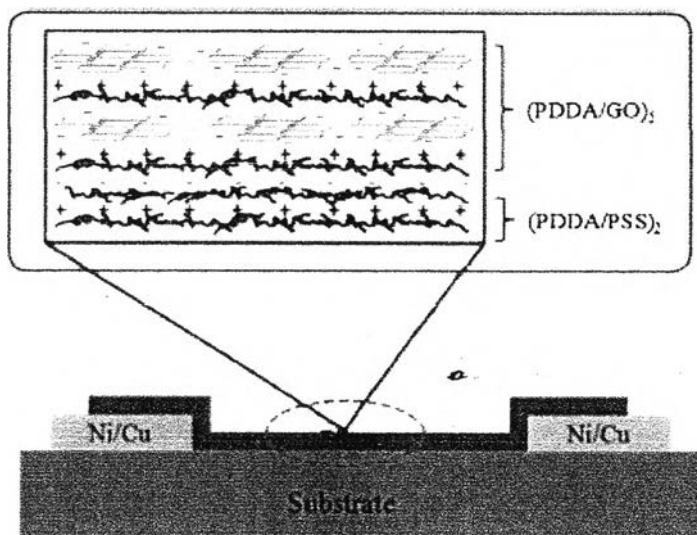


**Figure 2.10** LbL-assembled sensor of structure on sensing film.

## 2.5 Polymer solar cells (PSCs)

Polymer solar cells (PSCs) can be divided into conventional and inverted structures (Figure 2.11 a and b) according to the charge flow direction. A bulk-hetero-junction (BHJ) structure is usually adopted to construct a nanoscale interpenetrating network of a conjugated polymer donor and a fullerene derivative acceptor for the active layer in PSCs. The conventional BHJ PSCs are made from sandwiched structure between a modified transparent anode and a low work function (WF) metal cathode. Figure 2.11c illustrates the energy level and the main charge processes. When light pass through the transparent electrode , the photoactive layer was generated excitons diffusing towards and dissociate at the donor/acceptor interface into electrons in the lowest unoccupied molecular orbital (LUMO) of the acceptor material and holes in the highest occupied molecular orbital (HOMO) of the donor material. For enhancing the collection efficiency of holes on anode and electrons on cathode, WF of anode and cathode should be matched to the HOMO of donor and LOMO of acceptor,

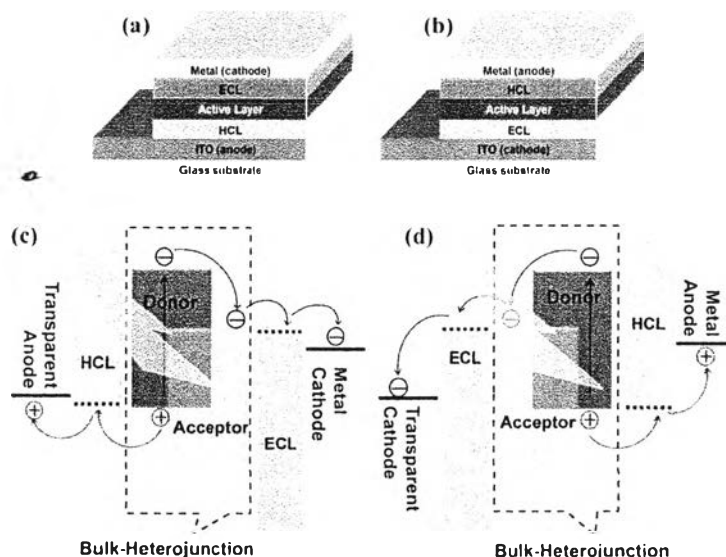


**Figure 2.11** Typical polymer solar cells (PSCs) structures of (a) conventional and (b) inverted PSCs. HCL: hole collection layer ; ECL: electron collection layer. Schematic illustration of the energy level and the charge transportation processes in (c) conventional and (d) inverted PSCs respectively (Fuzhi *et al.*, 2014).

Low WF metals as the top cathode have been selected for better matching with the LUMO acceptor. However, the low-work-function is not very stable as the top electrode due to degradation by oxygen and moisture in air, and the anode buffer layer (PEDOT:PSS) is acidic and corrosive to the ITO electrode.

Therefore, the concept of inverted polymer solar cells (see Figure 2.10b) has been introduced into PSCs to improve their long term stability. In inverted structure, the polarity of charge collection and charge flow direction are opposite to conventional structure, as shown in Figure 2.11d.

In 2014, Wenchao *et al.* published that a superior p-type organic HCL material should meet several requirements

(i) Processing solvent of the buffer layer should be orthogonal with that of active layer.

(ii) The state-of-the-art donor polymers often exhibited HOMO levels of 5.0 ~ 5.4 eV, and there by the work function of the p-type HCL material should exceed 5.0 eV to form ohmic contact with active layers.

(iii) The HCL should have very high transparency and thus the active layer can utilize more sunlight.

In 2014, Feng *et al.* presented a structural and morphological study of Poly[[4,8-bis[(2-ethylhexyl)oxy]benzo[1,2-b:4,5-b']dithiophene-2,6-diyl][3-fluoro-2-((2ethylhexyl) carbonyl) thieno[3,4-b] thiophenediyl]] (PTB7) and PC<sub>60</sub>BM - [6,6]-phenyl-C61-butyrac acid methylester (PC<sub>71</sub>BM) mixtures used as active layer in BHJ PSCs to elucidate the relationship between the morphology and device performance. They used diiodooctane (DIO) additive to prevent the large size PCBM aggregation of PTB7 at an early stage of the solution casting process, resulting in a finer size scale of the morphology and increased device efficiency.

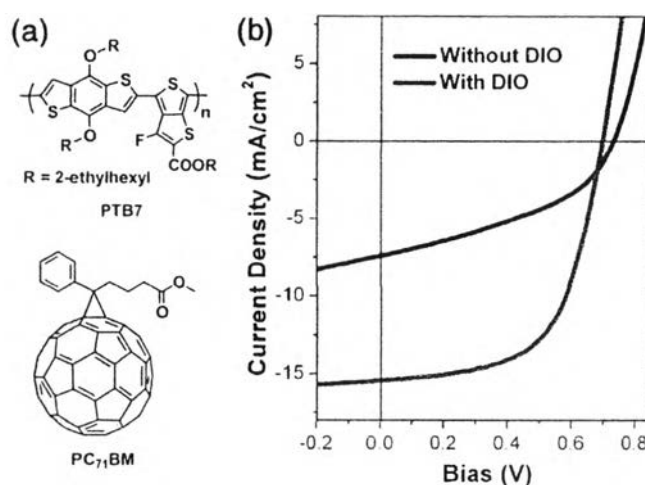


**Figure 2.12** a) Chemical structure of PTB7 and PC<sub>71</sub>BM. b) BHJ device performance processed with and without DIO additive, with chlorobenzene as the major solvent (Liu *et al.*, 2014).

In recent years, graphene oxide and reduced graphene oxide have been various interested in PSCs. In 2014, Tae-Woon *et al.* reported that a solution-processed RGO film can effectively serve as an interfacial material (IFL) for high performance inverted PSCs. The RGO was prepared with 4-(trifluoromethyl) phenylhydrazine reductant, which was recently introduced as an effective reductant to provide more improved conductivity, work function, and film uniformity than conventional hydrazine-based RGOs (Jin-Mun *et al.*, 2011). To increase water solubility of RGO, GO was reduce with hydrazine and simultaneous modification with poly(sodium 4-styrenesulfonate) (PSS) in Ngo *et al.* work in 2011.

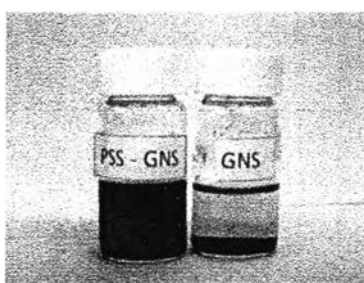


**Figure 2.13** The water dispersion (1 mg/ml) of graphene oxide nanosheet (GNS) and PSS-GNS after 1 month.

### 3 Conducting Polymers

The discovery of the first organic polymer that possesses metallic conductivity, polyacetylene, in 1977 has opened up possibilities for the development of a new class of materials known as intrinsically conducting polymers, or simply conducting polymers. In 2000, the Nobel prize for Chemistry was awarded to the three scientists who discovered polyacetylene (Alan G. MacDiarmid, Hideki Shirakawa, and Alan J. Heeger) “for the discovery and development of conducting polymers” Since then, a surge of research effort has been directed towards the development, synthesis and characterization of new types of conducting polymer materials. As a result, many different kinds of conducting polymers have been discovered and synthesized such as polyaniline, polypyrrole, polythiophene and poly(3,4-ethylenedioxythiophene) (PEDOT).

Polyaniline is one of the most known conducting polymers and has been extensively reviewed. It reported that polyaniline can be synthesized to various forms 1-dimensional nanostructures, including wires, rods, tubes and ribbons. Polyaniline has been studied for use in a wide range of applications such as chemical sensor, battery electrode, supercapacitors, fuel cells, polymer solar cells and separation membranes due to its environmental stability, redox reversibility, high electrical conductivity and ease of synthesis.

The two most important factors of chemical structure of polyaniline are redox state and the doping level. Polyaniline mainly has three types, namely, the fully reduced (leucoemeraldine), the half oxidized (emeraldine), and the fully oxidized (pernigraniline). In principle, polyaniline can exist in a continuum of oxidation states ranging from a completely reduced to a completely oxidized form. The chemical structure of polyaniline is shown in Figure 2.14.

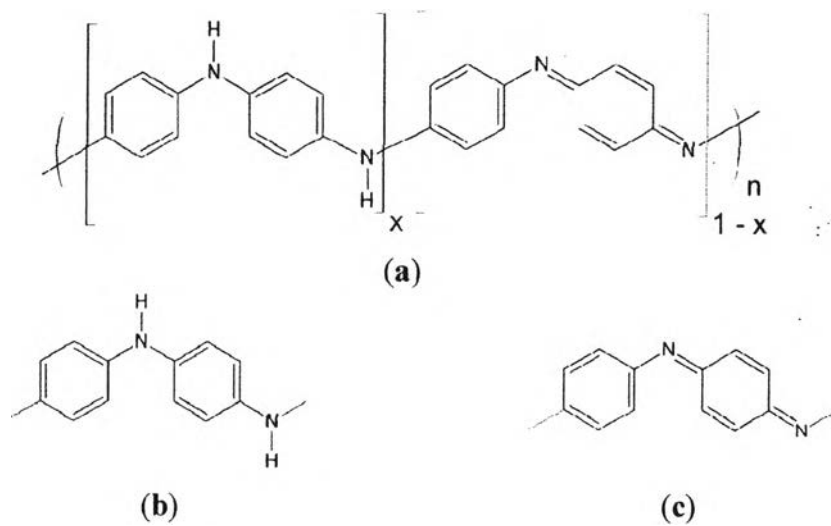


**Figure 2.14** The chemical structure of polyaniline and its repeating units. (a) A general chemical structure of polyaniline, (b) Reduced repeating unit, and (c) oxidized repeating unit.